ISSN 1068-3755, Surface Engineering and Applied Electrochemistry, 2025, Vol. 61, No. 5, pp. 686–691. © Allerton Press, Inc., 2025.
Russian Text © The Author(s), 2025, published in Elektronnaya Obrabotka Materialov, 2025, No. 5, pp. 79–84.

Structure, Elemental, and Phase Composition of the Surface Alloy Ti–Al–V–Ag Synthesized by the Combined Action of Ion-Plasma Flows

A. V. Basalai[a], *, N. N. Cherenda[b], A. Yu. Izobello[a], A. P. Laskovnev[a], V. V. Uglov[b], L. V. Bakhanovich[a], V. M. Astashinsky[c], and A. M. Kuzmitsky[c]

[a] *Physical-Technical Institute, National Academy of Sciences of Belarus, Minsk, 220084 Republic of Belarus*
[b] *Belarusian State University, Minsk, 220030 Republic of Belarus*
[c] *Lykov Institute of Heat and Mass Transfer, National Academy of Sciences of Belarus, Minsk, 220072 Republic of Belarus*
**e-mail: anna.basalay@mail.ru*

Received April 18, 2022

Abstract—The formation of surface Ti–Ag–Al–V alloy was carried out by compression plasma flows impact on Ti–6Al–4V titanium alloy preliminary coated by silver. The coating was deposited on the sample by the electron beam technique. The thickness of the coating was approximately 2 μm. The treatment of the system samples was carried out by three pulses of compression plasma flows in a nitrogen atmosphere (energy density absorbed by the surface varied from 26 to 43 J/cm^2 per pulse). The phase and elemental composition, structure, surface roughness, and microhardness were investigated. It has been established that the action of compression plasma flows on Ag/Ti–6Al–4V system results in the formation of TiAg, Ag, and δ-TiN in the surface alloyed layer. Increase of the energy absorbed by the surface during plasma impact (26–43 J/cm^2) led to a decrease in Ag concentration (20.0–6.9 wt %) in the analyzed layer. The change of phase composition and structure results in modification of the microhardness. A microhardness increase up to 4.8 GPa (1.3 times in comparison with initial Ti–6Al–4V alloy) was found after compression plasma flows' treatment at 43 J/cm^2.

Keywords: structure, phase composition, titanium alloy Ti–6Al–4V, silver, microhardness
DOI: 10.3103/S1068375525700747

INTRODUCTION

Titanium and its alloys are attracting increasing attention in the field of orthopedics and dentistry due to their strength properties, corrosion resistance, and biocompatibility [1]. However, the most widely used titanium alloy Ti–6Al–4V has some potential problems: the presence of toxic vanadium (V) or aluminum (Al). Bacterial infection is another major cause of failure of titanium implants. Even if the operation is performed under strict aseptic conditions, the average infection rate of orthopedic titanium implants reaches 5% [2]. Therefore, the development of titanium alloys with bactericidal properties is a pressing task.

The antimicrobial action of such metals as silver, copper, and zinc is widely known [3–7], including as part of coatings on implants. The introduction of these metals into the composition of the surface layer of implants can be carried out by electrochemical deposition, chemical vapor deposition, sputtering onto a substrate (magnetron sputtering, ion implantation), laser ablation, and the sol-gel method [8, 9]. Previous studies have shown that the effect of compressed plasma flows (CPF) on the coating-substrate system allows doping the surface layers of materials with coating atoms, providing a targeted change in the chemical composition, structure, and properties of the surface layer up to 40 μm deep [10].

Silver exhibits the greatest antibacterial properties. According to [11], the bactericidal effect is achieved by damaging cell membranes due to the adsorption of silver ions on cells. It is claimed in [12] that, when silver ions react with negatively charged nitrogen, oxygen, and sulfur, present in the form of phosphate, amino, carboxyl, and thiol groups in cellular proteins and bacterial DNA, a disruption in the functions of enzymes and nucleic acids occurs, which ultimately leads to damage to the bacterial DNA. Unlike antibiotics, which inhibit metabolic processes in bacteria, silver ions destroy the bacterial wall, which prevents bacteria from becoming accustomed to this bactericidal agent.

An analysis of literary data showed that the bactericidal properties of such materials depend not only on the concentration of silver but also on the state in which it is present in the material (metallic or oxide phase, solid solution, particles, or clusters) as well as on the surface topography. In addition, the use of

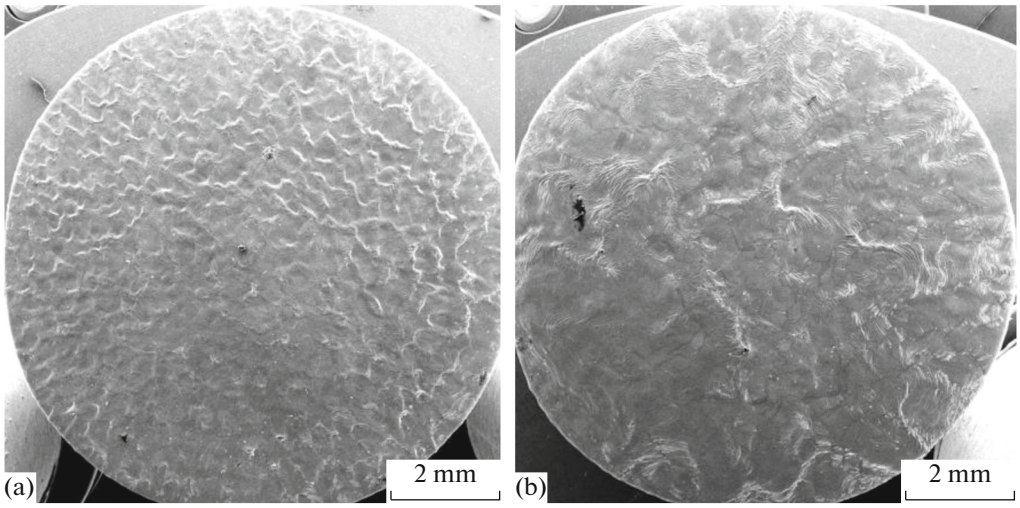

Fig. 1. SEM images of the sample surface Ag/Ti–6Al–4V systems after CPF exposure with the density of absorbed energy (a) $Q = 26$ J/cm^2 and (b) $Q = 43$ J/cm^2.

materials with a high silver content, which are known to have strong antibacterial activity, is limited by the possible toxic effect of silver ions on healthy cells of the body. It was found in [2] that, at a silver concentration of 26.7 wt %. In this regard, alloys were studied in this work where the silver concentration varied in the range (7–20 wt %) in order to minimize the possible toxic effect.

Thus, the aim of the work was to study the structure, elemental, and phase composition and properties of the surface layer of the Ti–6Al–4V alloy additionally alloyed with silver under the influence of CPF on the Ag/Ti–6Al–4V system.

MATERIALS AND METHODS

The formation of a titanium-based surface alloy containing silver was achieved by preliminary deposition of a silver coating with a thickness of ~2 μm on Ti–6Al–4V alloy samples using the electron beam method and subsequent exposure to CPF. As a result of plasma exposure, the coating and the surface layer of the substrate melt, liquid-phase mixing of the melt and its crystallization under conditions of ultrafast cooling occur [10]. The CPF samples were treated with three pulses at an initial capacitor bank voltage of 4 kV. The discharge duration was ~100 μs. Before the discharge, the preevacuated vacuum chamber of the compressor was filled with working gas (nitrogen) to a pressure of 400 Pa. The distance between the sample and the cathode cut of the electric discharge system varied in the range of 8–14 cm. An increase in this distance causes a decrease in the energy absorbed by the sample surface during plasma exposure, in the range of 26–43 J/cm^2. The surface morphology of the samples was studied using scanning electron microscopy (SEM) on a MIRA 3 LMH microscope. The elemental composition of the samples was determined by energy-dispersive X-ray microanalysis (EDXMA) using an Oxford Instruments detector coupled to a scanning electron microscope. The phase composition was studied by X-ray structural analysis using a RIGAKU Ultima IV diffractometer in parallel beam geometry in Cu-Kα radiation. The microhardness of the surface layers of the studied samples was determined using the Vickers method on a PMT-3 microhardness tester under a load of 1 N. Roughness parameters were determined using a base length of 0.8 mm using a Mahr MarSurf SD 26 profilometer.

RESULTS AND DISCUSSION

The effect of CPF on the surface of sample systems Ag/Ti–6Al–4V with different absorbed energy density leads to a change in its morphology (Fig. 1). The formation of wave-like structures oriented in the direction of plasma movement was established as a result of the melt spreading to the edges of the sample under the pressure of the plasma flow enveloping the sample. Increasing the density of absorbed energy with $Q =$ 26 J/cm^2 (Fig. 1a) to $Q = 43$ J/cm^2 (Fig. 1b) leads to the formation of less developed surface morphology.

According to literature data, bone implants with a rough surface have higher stability rates during twisting and pulling compared to smooth implants [13]. Application implants with a rough surface help to solve a number of problems: they allow for accelerated bone integration, a higher percentage of bone-implant contact and increased resistance to deformation, which is confirmed by a comparison of the torque values of a titanium implant with a polished or rough surface [13]. Results of research and theoretical calculations [14],

Table 1. Roughness parameters after CPF treatment on Ag/Ti–6Al–4V system

Roughness parameters	After exposure to CPF at different energy densities Q			
	26 J/cm^2	30 J/cm^2	37 J/cm^2	43 J/cm^2
Ra, μm	1.4	1.3	1.3	1.1
R_z, μm	7.8	7.1	6.9	6.1
R_{max}, μm	11.9	10.3	9.8	8.1

Table 2. Concentration of elements in the surface layer before and after CPF exposure to the Ag/Ti–6Al–4V system, wt %

System under study	Energy density Q, J/cm^2	Concentration of elements, wt %				
		Ti	Al	V	Ag	N
Ti–6Al–4V	–	89.9	6.1	4.0	–	–
Ag/Ti–6Al–4V	26	66.5	2.7	2.3	20.0	8.5
	30	69.1	3.7	3.1	16.8	7.3
	37	75.3	4.0	3.4	10.3	7.0
	43	79.1	4.1	3.5	6.9	6.4

which evaluated implants with different surface topographies, showed that improved bone formation was observed when the roughness value was $Ra = 1.5$ μm.

As can be seen from the presented results (Table 1), surface roughness parameter Ra varied from 1.1 to 1.5 μm, with an increase in the density of absorbed energy accompanied by a decrease in surface roughness. Thus, the effect of CPF allows us to obtain a developed surface morphology with an optimal value Ra, which makes such complex treatment promising for dental and orthopedic implants.

The study of the elemental composition of the surface layer with a thickness of ~1 μm using energy dispersive microanalysis showed that silver and nitrogen atoms (as a plasma-forming gas) are present in the surface layer of the titanium alloy after the deposition of the silver coating and subsequent exposure to CPF. Increase in energy density from 26 to 43 J/cm^2 is accompanied by a decrease in the concentration of Ag from 20.0 to 6.9 wt %. The concentration of nitrogen in the surface layer decreases with an increase in the absorbed energy density from 8.5 to 6.4%. The decrease in the concentration of the additional alloying element (Ag) with an increase in the absorbed energy density can be due to several factors. The increase in energy density is accompanied by an increase in the temperature of the surface layer of the titanium alloy, thereby ensuring the heating of deeper layers to the melting temperature, which leads to alloying of deeper layers. At the same time, due to the redistribution of the alloying element throughout the entire layer, its concentration decreases. In addition, erosion of the material surface contributes to a decrease in the concentration of the alloying element in the surface layer with an increase in energy density.

The action of CPF on Ti–6Al–4V alloy with preapplied Ag coating allows for the formation of a surface layer with reduced content of toxic V and Al. The original sample containing aluminum and vanadium (Table 2) corresponds to the grade composition for the Ti–6Al–4V alloy [15]. The application of a silver coating and subsequent exposure to CPF is accompanied by a decrease in the concentration of the main alloying elements of the alloy in the surface layer, which is due to the introduction of an additional coating element (Ag) and plasma-forming gas (N) into the remelted surface layer as a result of exposure to CPF. Moreover, lower CPF processing energy density corresponds to lower concentrations of aluminum and vanadium. A significant decrease in the concentration of aluminum (up to 2.3 times) in the studied alloy after exposure to CPF may be associated with its intense evaporation due to the relatively low boiling point. It is also indicated in [16] that the concentration of Al decreases when electron beams are applied to the Ti–6Al–4V alloy.

The results of the phase composition analysis of the initial sample of titanium alloy Ti–6Al–4V and the Ag/Ti–6Al–4V system after exposure to CPF are presented in Fig. 2. In the original coated sample, the diffraction lines of α-Ti are shifted towards smaller diffraction angles relative to the standard since the main phase of the Ti–6Al–4V alloy is the substitution solid solution α-Ti (Al, V). The diffraction pattern of the original sample shows a diffraction line of vanadium V(110) at $2\theta = 41.9°$.

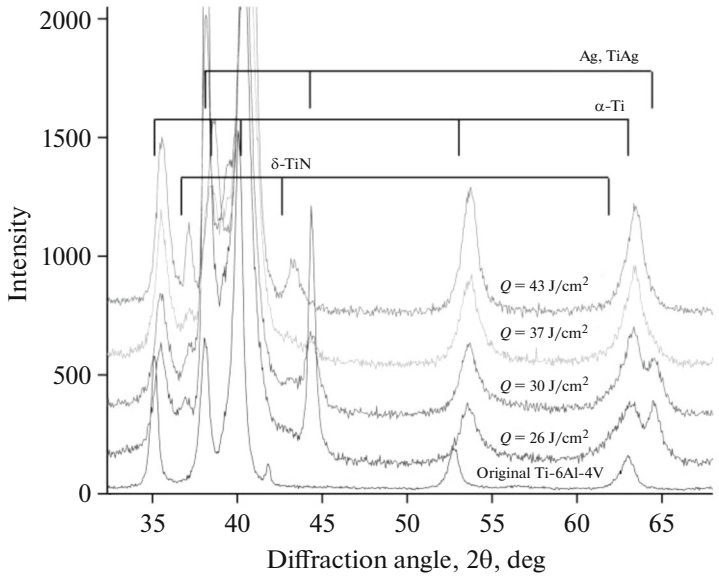

Fig. 2. Sections of the diffraction patterns of the original sample of Ti–6Al–4V alloy and the Ag/Ti–6Al–4V system after exposure to CPF.

When CPF acts on the Ag/Ti–6Al–4V system, vanadium precipitates dissolve. The vanadium diffraction line is absent under all exposure conditions. With increasing energy and decreasing silver concentration, vanadium atoms can enter into the composition of a supersaturated solid solution based on the α-phase, exerting a decisive influence on its lattice parameter (vanadium atoms have a smaller radius than titanium atoms). However, one cannot exclude the possibility of the formation of dispersed vanadium precipitates that cannot be recorded by X-ray structural analysis.

After alloying the surface layer of the titanium alloy with silver, lines are observed in the diffraction pattern that may belong to both Ag and the TiAg phase with interplanar distances close to Ag. The presented data correlate with the results of studies of the properties of biomedical materials made of Ti–6Al–4V alloy in the process of immersion ion implantation of silver [6]. It was established in [6] that the layer with the modified surface contains Ag and TiAg. The volume fraction of formed phases decreases with increasing absorbed energy density. At the absorbed energy density Q = 43 J/cm^2 and, as a consequence, with a decrease in the concentration of silver (Table 2), diffraction lines corresponding to the TiAg and Ag phases are absent.

As a result of the interaction of CPF, the plasma-forming gas of which is nitrogen, with the Ag/Ti–6Al–4V system, titanium nitride δ-TiN is formed in the surface layer. As can be seen from the presented data, an increase in the density of absorbed energy is accompanied by an increase in the volume fraction of the titanium nitride phase.

The formation of a nitride film on the surface of the samples under study is confirmed by scanning electron microscopy data (Fig. 3). It is evident in Fig. 3 that exposure to CPF is characterized by the formation of a dendritic structure, which can be caused by both thermal and concentration supercooling. During rapid cooling under nonequilibrium conditions, the composition of the resulting solid phase differs from the composition of the liquid from which it was formed; this leads to the emergence of a concentration gradient in the liquid ahead of the crystallization front, i.e., concentration supercooling occurs, which determines the growth structures in alloys. The formation of a dendritic structure depends on the magnitude of supercooling and, consequently, on the temperature gradient in the liquid, the speed of movement of the crystallization front, and the initial concentration of impurity in the melt. The grain size of the formed structure is approximately 0.5 μm Q = 26 J/cm^2. With increase of Q up to 43 J/cm^2, the size increases to ~1 μm. Formation of similar dendritic structures has previously been observed during nitriding of technical grade titanium alloy using CPF [17].

The above described changes in the elemental and phase composition, structure, and surface topography, when CPF is applied to titanium alloy Ti–6Al–4V with a preapplied silver coating, lead to an increase in the microhardness of the surface layer (Fig. 4).

An increase in the microhardness of the surface layer is observed for all CPF exposure modes. This is explained by the effects of rapid quenching, in particular, the dispersion of the structure, the formation of titanium nitride, an intermetallic compound, and a change in the concentration of alloying elements in the titanium solid solution. An increase in the density of absorbed energy is accompanied by an increase in

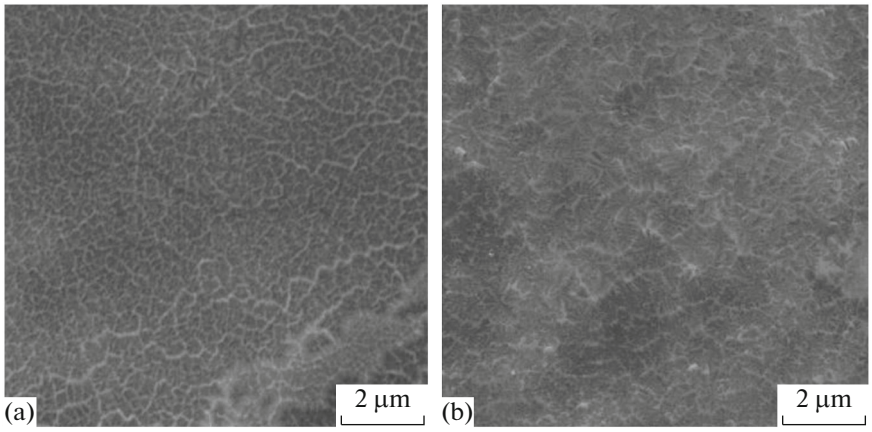

Fig. 3. SEM images of the Ag/Ti–6Al–4V sample surface after CPF exposure with the density of absorbed energy (a) Q = 26 J/cm^2 and (b) Q = 43 J/cm^2.

microhardness. The maximum microhardness value reaches 4.8 GPa when exposed to CPF with an absorbed energy density of Q = 43 J/cm^2, which corresponds to an increase in microhardness by 1.3 times compared to the original sample. According to the X-ray structural analysis data, the volume fraction of titanium nitride increases with the increase of the absorbed energy density of the CPF impact on the titanium alloy with a preapplied coating; therefore, the formation of nitride can have a predominant effect on the change in the microhardness of the surface layer compared to the titanium alloy, which explains the obtained nature of the dependence of the change in microhardness. In addition, an increase in microhardness with an increase in the density of absorbed energy can be due to a higher concentration of alloying (strengthening) elements of the alloy (Al and V) in the α-Ti solid solution.

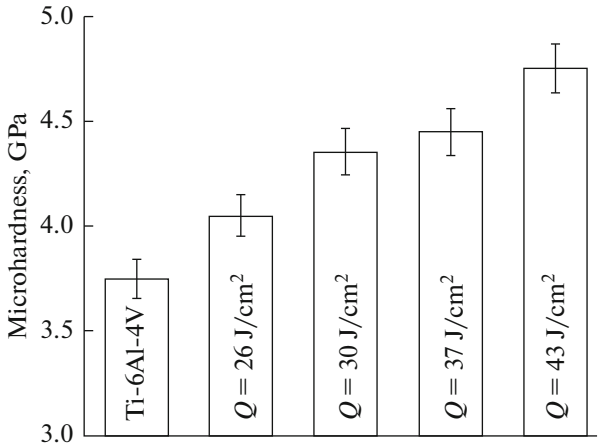

Fig. 4. Microhardness of the surface layer of the original sample of titanium alloy Ti–6Al–4V and samples of the Ag/Ti–6Al–4V system after exposure to CPF depending on the modes.

CONCLUSIONS

It has been established that exposure to three CPF pulses at Q = 26–43 J/cm^2 on Ti–6Al–4V with a preapplied silver coating is accompanied by the formation of a surface alloy based on titanium, silver, aluminum, and vanadium containing nitrogen atoms. The structure, phase, and elemental composition of the formed surface alloy, as well as the microhardness, depend on the energy absorbed by the surface of the sample. As the density of absorbed energy increases, the content of silver and nitrogen decreases. The effect of CPF on the Ag/Ti–6Al–4V system is accompanied by the formation δ-TiN, TiAg, Ag, and solid solution based on α-Ti. With increasing energy density, the volume fraction of the δ-TiN phase increases, while the TiAg and Ag phases decrease, and TiAg and Ag phases are not observed at Q = 43 J/cm^2. CPF treatment of the studied system leads to an increase in microhardness by 1.1 and 1.3 times compared to the original sample. Possible reasons for the increase in microhardness are the formation of nitride phases, dispersion of the structure, and changes in the concentration of alloying (strengthening) elements of the alloy (Al and V) in the α-Ti solid solution. An increase in the density of absorbed energy is accompanied by an increase in microhardness.

FUNDING

This work was supported by ongoing institutional funding. No additional grants to carry out or direct this particular research were obtained.

CONFLICT OF INTEREST

The authors of this work declare that they have no conflicts of interest.

REFERENCES

1. Banerjee, D. and Williams, J.C., Perspectives on titanium science and technology, *Acta Mater.,* 2013, vol. 61, no. 3, p. 844.
2. Sukhorukova, I.V., Creation of bioactive coatings Ti-CaPCON/(Ag, AUGMENTIN) with antibacterial effect, *Cand. Sci. (Eng.) Dissertation),* Moscow: MISIS, 2015.
3. Kang, M.K., Moon, S.K., Kwon, J.S., Kim, K.M., et al., Antibacterial effect of sand blasted, large-grit, acid-etched treated Ti–Ag alloys, *Mater. Res. Bull.,* 2012, vol. 47, no. 10, p. 2952.
4. Lei, Z., Zhang, H., Zhang, E., You, J., et al., Antibacterial activities and biocompatibilities of Ti–Ag alloys prepared by spark plasma sintering and acid etching, *Mater. Sci. Eng.,* 2018, vol. 92, p. 121.
5. Maharubin, Sh., Hu, Y., Sooriyaarachchi, D., Cong, C., et al., Laser engineered net shaping of antimicrobial and biocompatible titanium-silver alloys, *Mater. Sci. Eng.,* 2019, vol. 105, p. 110.
6. Liu, H., Xu, Q., Zhang, X., Wang, C., et al., Wear and corrosion behaviors of Ti6Al4V alloy biomedical materials by silver plasma immersion ion implantation process, *Thin Solid Films,* 2012, vol. 521, p. 89.
7. Fowler, L., Janson, O., Engqvist, H., Norgren, S., et al., Antibacterial investigation of titanium-copper alloys using luminescent Staphylococcus epidermidis in a direct contact test, *Mater. Sci. Eng.,* 2019, vol. 97, p. 707.
8. Vasil'ev, M.A., Nishchenko, M.M., and Gurin, P.A., Laser modification of the surface of titanium implants, *Usp. Fiz. Met.,* 2010, vol. 11, p. 209.
9. Lei, M.K., Dong, Z.H., Zhang, Z., Hu, Y.F., et al., Wear and corrosion resistance of Ti–6Al–4V alloy irradiated by high-intensity pulsed ion beam, *Surf. Coat. Technol.,* 2007, vol. 201, nos. 9–11, p. 5613.
10. Uglov, V.V., Cherenda, N.N., Anishchik, V.M., Astashinskii, V.M., and Kvasov, N.T., *Modifikatsiya materialov kompressionnymi plazmennymi potokami* (Modification of Materials by Compression Plasma Flows), Minsk: Belarus. Gos. Univ., 2013.
11. Marambio-Jones, C. and Hoek, E.M.V., A review of the antibacterial effects of silver nanomaterials and potential implications for human health and the environment, *J. Nanopart. Res.,* 2010, vol. 12, no. 5, p. 1531.
12. Chernousova, S. and Epple, M., Silver as antibacterial agent: Ion, nanoparticle, and metal, *Angew. Chem. Int. Ed.,* 2013, vol. 52, no. 6, p. 1636.
13. Perikova, M.G., Clinical and laboratory substantiation of screw dental implants with developed surface topography and bioactive surface properties, *Cand. Sci. (Med.) Dissertation,* Volgograd, 2014.
14. Cooper, L.F., The role of surface topography in bone regeneration and preservation during the installation of titanium endosseous dental implants, *Nov. Stomatol.,* 2008, no. 8, p. 83.
15. Kolachev, B.A., Pol'kin, I.S., and Talalaev, V.D., *Titanovye splavy raznykh stran* (Titanium Alloys of Different Countries), Moscow: VILS, 2000.
16. Belov, A.B., Bytsenko, O.A., Krainikov, A.V., et al., *Sil'notochnye impul'snye elektronnye puchki dlya aviatsionnogo dvigatelestroeniya* (High-Current Pulsed Electron Beams for Aircraft Engine Building), Moscow: Dipak, 2012.
17. Astashinskii, V.M., Uglov, V.V., Cherenda, N.N., and Shimanskii, V.I., *Modifikatsiya titana pri vozdeistvii kompressionnymi plazmennymi potokami* (Modification of Titanium by Exposure to Compression Plasma Flows), Minsk: Belaruskaya Navuka, 2016.